A fast and long-lived outflow from the supermassive black hole in NGC 5548

J. S. Kaastra,[1,2,3]* G. A. Kriss,[4,5] M. Cappi,[6] M. Mehdipour,[1,7] P.-O. Petrucci,[8,9] K. C. Steenbrugge,[10,11] N. Arav,[12] E. Behar,[13] S. Bianchi,[14] R. Boissay,[15] G. Branduardi-Raymont,[7] C. Chamberlain,[12] E. Costantini,[1] J. C. Ely,[4] J. Ebrero,[1,16] L. Di Gesu,[1] F. A. Harrison,[17] S. Kaspi,[13] J. Malzac,[18,19] B. De Marco,[20] G. Matt,[14] K. Nandra,[20] S. Paltani,[15] R. Person,[21] B. M. Peterson,[22,23] C. Pinto,[24] G. Ponti,[20] F. Pozo Nuñez,[25] A. De Rosa,[26] H. Seta,[27,28] F. Ursini,[8,9] C. P. de Vries,[1] D. J. Walton,[17] M. Whewell[7]

[1]SRON Netherlands Institute for Space Research, Sorbonnelaan 2, 3584 CA Utrecht, Netherlands. [2]Department of Physics and Astronomy, Universiteit Utrecht, P.O. Box 80000, 3508 TA Utrecht, Netherlands. [3]Leiden Observatory, Leiden University, PO Box 9513, 2300 RA Leiden, Netherlands. [4]Space Telescope Science Institute, 3700 San Martin Drive, Baltimore, MD 21218, USA. [5]Department of Physics and Astronomy, Johns Hopkins University, Baltimore, MD 21218, USA. [6]INAF-IASF Bologna, Via Gobetti 101, I-40129 Bologna, Italy. [7]Mullard Space Science Laboratory, University College London, Holmbury St. Mary, Dorking, Surrey, RH5 6NT, UK. [8]Univ. Grenoble Alpes, IPAG, F-38000 Grenoble, France. [9]CNRS, IPAG, F-38000 Grenoble, France. [10]Instituto de Astronomía, Universidad Católica del Norte, Avenida Angamos 0610, Casilla 1280, Antofagasta, Chile. [11]Department of Physics, University of Oxford, Keble Road, Oxford, OX1 3RH, UK. [12]Department of Physics, Virginia Tech, Blacksburg, VA 24061, USA. [13]Department of Physics, Technion-Israel Institute of Technology, 32000 Haifa, Israel. [14]Dipartimento di Matematica e Fisica, Università degli Studi Roma Tre, via della Vasca Navale 84, 00146 Roma, Italy. [15]Department of Astronomy, University of Geneva, 16 Ch. d'Ecogia, 1290 Versoix, Switzerland. [16]European Space Astronomy Centre (ESAC), P.O. Box 78, E-28691 Villanueva de la Cañada, Madrid, Spain. [17]Cahill Center for Astronomy and Astrophysics, California Institute of Technology, Pasadena, CA 91125, USA. [18]Université de Toulouse, UPS-OMP, IRAP, Toulouse, France. [19]CNRS, IRAP, 9 Av. colonel Roche, BP 44346, 31028 Toulouse Cedex 4, France. [20]Max-Planck-Institut für extraterrestrische Physik, Giessenbachstrasse, D-85748 Garching, Germany. [21]22 Impasse du Bois Joli, 74410 St. Jorioz, France. [22]Department of Astronomy, The Ohio State University, 140 W 18th Avenue, Columbus, OH 43210, USA. [23]Center for Cosmology & AstroParticle Physics, The Ohio State University, 191 West Woodruff Avenue, Columbus, OH 43210, USA. [24]Institute of Astronomy, University of Cambridge, Madingley Rd, Cambridge, CB3 0HA, UK. [25]Astronomisches Institut, Ruhr-Universität Bochum, Universitätsstraße 150, 44801, Bochum, Germany. [26]INAF/IAPS - Via Fosso del Cavaliere 100, I-00133 Roma, Italy. [27]Research Center for Measurement in Advanced Science, Faculty of Science, Rikkyo University 3-34-1 Nishi-Ikebukuro, Toshima-ku, Tokyo, Japan. [28]Department of Physics, Saitama University, 255 Shimo-Okubo, Sakura-ku, Saitama 338-8570, Japan.

*Corresponding author. E-mail: J.Kaastra@sron.nl

Supermassive black holes in the nuclei of active galaxies expel large amounts of matter through powerful winds of ionized gas. The archetypal active galaxy NGC 5548 has been studied for decades, and high-resolution x-ray and UV observations have previously shown a persistent ionized outflow. An observing campaign in 2013 with six space observatories shows the nucleus to be obscured by a long-lasting, clumpy stream of ionized gas never seen before. It blocks 90% of the soft x-ray emission and causes simultaneous deep, broad UV absorption troughs. The outflow velocities of this gas are up to five times faster than those in the persistent outflow, and at a distance of only a few light days from the nucleus, it may likely originate from the accretion disk.

Outflows of photo-ionized gas are ubiquitous in active galactic nuclei (AGN) such as Seyfert galaxies (*1*, *2*). Their impact on the environment can be estimated from the mass loss rate per solid angle, which is proportional to the hydrogen column density $N_{\rm H}$, outflow velocity v and distance r to the ionizing source. While the first two quantities are directly obtained from high-resolution spectral observations, in most cases the distance can only be inferred from the ionization parameter $\xi=L/nr^2$, with n being the hydrogen density and L the ionizing luminosity between 13.6 eV and 13.6 keV. The density can be obtained from density-sensitive UV lines or by measuring the recombination time scale $t_{\rm rec}\sim 1/n$ by monitoring the response of the outflow to continuum variations. The latter approach has recently been successfully applied to Mrk 509, providing strong constraints on the distances of the five ionization components in that source (*3*, *4*).

Motivated by the successful results of the Mrk 509 campaign, we have conducted comprehensive monitoring of NGC 5548, an archetypal Seyfert 1 galaxy (z=0.017175). This campaign from May 2013 to February 2014 involved observations with the XMM-Newton, Hubble Space telescope (HST), Swift, the Nuclear Spectroscopic Telescope Array (NuSTAR), the INTErnational Gamma-Ray Astrophysics Laboratory (INTEGRAL), and Chandra satellites (*5*).

To our surprise, the soft X-ray flux in the first XMM-Newton observation (22 June 2013) was 25 times weaker than the typical median as measured with Chandra LETGS in 2002, and this strong suppression was consistent throughout all 14 XMM-Newton spectra (Fig. 1). The NuSTAR and INTEGRAL spectra at energies above 10 keV show the characteristic power-law shape with a photon index of 1.6–1.7 and a weak constant reflection component, consistent with the median flux level of the 2002 Chandra/LETGS observation. However, the spectrum is cut off below 10 keV, reaching an effective photon index of −0.5 in the 1–2 keV band, before it flattens again below 1 keV. At energies <1 keV, the spectrum shows clear narrow emission lines and radiative recombination continua from photoionized gas at a temperature of ~6 eV. The intensity of the strongest emission line, the [O VII] forbidden line at 0.56 keV, is only slightly below its 2002 intensity. These narrow features are superimposed on a weak continuum.
Comptonized spectra cannot explain the observed hard photon index. The central continuum is more likely absorbed by obscuring material that partially covers (~90%) the source. The absorbing gas must be inside the X-ray narrow line region; we concluded that this region is not obscured, because the intensity of the narrow emission features is not suppressed compared to archival data.

We obtained HST/COS spectra concurrently with six of our 14 XMM-Newton spectra (Fig. 1). These UV spectra show a large number of narrow absorption lines at the velocities of the classical warm absorber (WA) components that were already present 20 years ago (*1*), but which now originate from less-ionized gas. This shows that the WA is now irradiated by a much lower ionizing flux than before.

After modeling the emission lines and continuum and accounting for the narrow absorption lines from the WA (*5*), broad, blue-shifted absorption troughs remain visible in the COS spectra (Fig. 2). Asymmetric troughs reach their deepest point at outflow velocities of −1000 km/s and extend to blueshifts as high as −5000 km/s. All permitted UV transitions in the COS spectra show this blueshifted absorption: C II, Si II, Si II*, S II, Fe III, C III*, Si III, Si IV, C IV, N V, and Lyα. As expected, no absorption is seen associated with forbidden or semi-forbidden transitions, or highly excited states such as He II λ1640. As we show below, all visible broad absorption transitions appear in ions formed at ionization parameters similar to those needed to explain the X-ray obscuration. In addition, there is a hint of a correlation between the strengths of the broad absorption troughs in the individual observations with the strength of the X-ray obscuration (Fig. 2C), which may suggest that the broad UV absorption troughs and the X-ray obscuration arise in the same photoionized gas.

As indicated above, the UV manifestation of the persistent classical WA has a significantly lower degree of ionization due to this obscuration. Lower ionization will also cause a significant increase in the X-ray opacity of the WA that needs to be taken into account when modeling the obscuring medium in the X-ray band. Therefore we developed a proper model for the 2013 WA (*5*) based on the physical characteristics of the WA and SED as measured in 2002 (*6*), when there was no obscurer present.

The best-fit model with a single obscuring component produced a very hard continuum spectrum with a photon index of 1.48, inconsistent with the high-energy NuSTAR data that are not affected by obscuration. We required two obscuring components to find a solution consistent with the hard X-ray spectrum (Fig. S3), which has a photon index of 1.57.

The first obscuring component covers 86% of the X-ray source and has a hydrogen column density of 1.2×10^{26} m^{-2} and $\log \xi = -1.2$ (in units of 10^{-9} Wm). This component, derived from X-ray analysis only, reproduces all the broad absorption troughs seen in the UV. The similar depths of the red and blue transitions for Si IV, C IV, and N V in Fig. 2A indicate that the troughs are saturated. They only partially cover the broad lines and continuum, such that the line profiles indicate the velocity-dependent covering factor rather than the column density profile.

The troughs in C IV and Lyα are deep enough to fully cover the continuum emission, but it is not possible to unambiguously determine the separate broad-line and continuum covering fractions. If the continuum is fully covered, then the covering factor of the C IV BLR is 20%. For N V and Si IV the maximum continuum covering fractions are 95% and 40%, respectively. For continuum covering fractions of 30% in each line, the BLR covering fractions of C IV, N V and Si IV are 30%, 40%, and 20%, respectively. The signal in the RGS soft X-ray band is too low and dominated by features from the narrow emission lines and warm absorber to allow useful constraints on outflow velocity or line width of the obscurer. Therefore the COS UV spectra are essential for understanding the dynamics of the outflow.

The second obscuring component covers 30% of the X-ray source with $N_H = 10^{27}$ m^{-2} and is almost neutral. Taking the same ratio between the X-ray and the UV continuum covering factors as for component 1 (86% for X-ray, 30% for UV), the UV covering factor of component 2 is small (less than 10%).

The obscuration is present during our full campaign – see Fig. 3. Archival Swift data (Fig. S4) show large hardness ratios, a strong signature of photoelectric absorption, indicating the obscuration started between August 2007 and February 2012, when Swift was not monitoring NGC 5548; a HST/COS spectrum taken in June 2011 already indicates an onset of the broad absorption lines. Thus the obscuration has lasted for at least 2.5 years, and perhaps as long as six years.

Interestingly, in early September 2013, NGC 5548 brightened for about two weeks (Fig. 3). The Swift X-ray hardness ratio indicated that the source was still obscured, so the continuum itself must have increased. The last Chandra LETGS spectrum of 11 September 2013 showed the effect of the outburst as an increase in the ionization degree of the WA and re-appearance of several X-ray lines from the WA, but no noticeable effect on the obscurer.

What is the obscurer and where is it located (Fig. 4)? The UV troughs are deeper than the continuum, and the obscurer partially covers the broad UV emission lines, implying a distance of more than 2−7 light days (10^{14} m) from the core (*7*). However, it strongly affects the WA by reducing the level of ionization, implying the obscurer is within $\sim 10^{17}$ m from the core (*20*). Given the UV broad line covering factor of obscurer component 1 of 20–40%, it is likely that the obscurer is close to the broad UV line-emitting region. Based on the UV/X-ray ratio of continuum covering factors determined before for the obscuring component 1, it follows that the UV source is only two times larger than the X-ray source. Another indication for a distance just outside of the broad line region (BLR) is the high velocity of the gas in the line of sight, peaking at −1000 km/s and extending out to −5000 km/s. We see variations in the obscuration between subsequent XMM-Newton observations, spaced by two days. Assuming that the X-ray source has a typical size of $10R_g$ ($R_g = GM/c^2$) and a black hole mass $M = 3.9 \times 10^7$ solar masses (*8*), the velocity needed to cross this distance in two days is 3000 km/s, of the same order of magnitude as the velocities observed along the line of sight. On the other hand, this obscuration lasts for several years, indicating ongoing replenishment of the obscuring material, possibly from the accretion disk or from the BLR.

Given the location, the outflow velocity, and the changes in the X-ray covering fraction of the obscurer, we may attribute the obscuring material to a wind from the accretion disk reaching beyond the BLR. The line of sight is inclined by ~30° to the rotation axis of the disk (*8*), and these velocity components therefore indicate a predominantly poloidal outflow. This is more readily explained by magnetically confined acceleration than by radiative acceleration, which would lead to a more radial or equatorial outflow.

Evidence is accumulating for strong variations in the X-ray absorption properties along the line of sight for both type-1 and type-2 AGNs. X-ray absorbers show changes from Compton-thin to Compton-thick columns, changes in covering fraction, eclipse/occultation events, variations in the ionization state, and velocity of some of their major components (*9*–*17*). Observations so far suggest that these examples of circumnuclear absorbing gas are inhomogeneous and clumpy, preferentially distributed along the equatorial plane, and possibly due to either a clumpy torus or clouds of the BLR passing along the line of sight. On the other hand, the distant WA seems to persist over much longer time scales.

Compared with previous studies, our observations of this type-1 AGN stand out because i) this persistent X-ray/UV obscuring event implies a long, inhomogeneous stream of matter, possibly the onset of an accretion disc wind, and ii) this phenomenon was detected simultaneously in X-rays and UV.

Outflows powerful enough to influence their environments are present in luminous quasars like BAL QSOs. Theoretical models of radiatively driven accretion-disk winds in BAL QSOs require that the accelerated UV-absorbing gas is shielded from much of the UV/X-ray ionizing radiation (*18*). They predict heavy X-ray obscuration and broad UV absorption lines arising from gas near the accretion disk. Observational evidence is ambiguous, as (*19*) see evidence for both X-ray absorption and intrinsically weak X-ray emission in BAL QSOs.

The proximity and brightness of nearby Seyfert galaxies make them ideal laboratories for studying the mechanisms that drive the powerful winds seen in their more luminous cousins.

Our observations of NGC 5548 show that the X-ray obscuration and the fast broad UV outflow both arise in the region expected for an accretion disk wind, and we established that this shielding gas is near the broad-line region.

Although the outflow in NGC 5548 is not strong enough to influence its host galaxy, it gives us unique insight into how the same mechanism may be at work in much more powerful quasars.

References and Notes

1. C. S. Reynolds, An X-ray spectral study of 24 type 1 active galactic nuclei. *Mon. Not. R. Acad. Sci.* **286**, 513–537 (1997). doi:10.1093/mnras/286.3.513
2. D. M. Crenshaw, S. B. Kraemer, A. Boggess, S. P. Maran, R. F. Mushotzky, C.-C. Wu, Intrinsic absorption lines in Seyfert 1 galaxies. I. Ultraviolet Spectra from the *Hubble Space Telescope*. *Astrophys. J.* **516**, 750–768 (1999). doi:10.1086/307144
3. J. S. Kaastra, P.-O. Petrucci, M. Cappi, N. Arav, E. Behar, S. Bianchi, J. Bloom, A. J. Blustin, G. Branduardi-Raymont, E. Costantini, M. Dadina, R. G. Detmers, J. Ebrero, P. G. Jonker, C. Klein, G. A. Kriss, P. Lubiński, J. Malzac, M. Mehdipour, S. Paltani, C. Pinto, G. Ponti, E. M. Ratti, R. A. N. Smith, K. C. Steenbrugge, C. P. de Vries, Multiwavelength campaign on Mrk 509. *Astron. Astrophys.* **534**, A36 (2011). doi:10.1051/0004-6361/201116869
4. J. S. Kaastra, R. G. Detmers, M. Mehdipour, N. Arav, E. Behar, S. Bianchi, G. Branduardi-Raymont, M. Cappi, E. Costantini, J. Ebrero, G. A. Kriss, S. Paltani, P.-O. Petrucci, C. Pinto, G. Ponti, K. C. Steenbrugge, C. P. de Vries, Multiwavelength campaign on Mrk 509. *Astron. Astrophys.* **539**, A117 (2012). doi:10.1051/0004-6361/201118161
5. See supplementary materials on *Science* Online.
6. K. C. Steenbrugge, J. S. Kaastra, D. M. Crenshaw, S. B. Kraemer, N. Arav, I. M. George, D. A. Liedahl, R. L. J. van der Meer, F. B. S. Paerels, T. J. Turner, T. Yaqoob, Simultaneous X-ray and UV spectroscopy of the Seyfert galaxy NGC 5548. *Astron. Astrophys.* **434**, 569–584 (2005). doi:10.1051/0004-6361:20047138
7. K. T. Korista, D. Alloin, P. Barr, J. Clavel, R. D. Cohen, D. M. Crenshaw, I. N. Evans, K. Horne, A. P. Koratkar, G. A. Kriss, J. H. Krolik, M. A. Malkan, S. L. Morris, H. Netzer, P. T. O'Brien, B. M. Peterson, G. A. Reichert, P. M. Rodriguez-Pascual, W. Wamsteker, K. S. J. Anderson, D. J. Axon, E. Benitez, P. Berlind, R. Bertram, J. H. J. Blackwell, N. G. Bochkarev, C. Boisson, M. Carini, R. Carrillo, T. E. Carone, F.-Z. Cheng, J. A. Christensen, K. K. Chuvaev, M. Dietrich, J. J. Dokter, V. Doroshenko, D. Dultzin-Hacyan, M. N. England, B. R. Espey, A. V. Filippenko, C. M. Gaskell, M. R. Goad, L. C. Ho, J. P. Huchra, X. J. Jiang, S. Kaspi, W. Kollatschny, A. Laor, J.-P. Luminet, G. M. MacAlpine, J. W. MacKenty, Y. F. Malkov, D. Maoz, P. G. Martin, T. Matheson, B. McCollum, N. Merkulova, L. Metik, M. Mignoli, H. R. Miller, M. G. Pastoriza, D. Pelat, J. Penfold, M. Perez, G. C. Perola, J. L. Persaud, J. Peters, R. Pitts, R. W. Pogge, I. Pronik, V. I. Pronik, R. L. Ptak, L. Rawley, M. C. Recondo-Gonzalez, J. M. Rodriguez-Espinosa, W. Romanishin, A. C. Sadun, I. Salamanca, M. Santos-Lleo, K. Sekiguchi, S. G. Sergeev, A. I. Shapovalova, J. C. Shields, C. Shrader, J. M. Shull, N. A. Silbermann, M. L. Sitko, D. R. Skillman, H. A. Smith, S. M. Smith, M. A. J. Snijders, L. S. Sparke, G. M. Stirpe, R. E. Stoner, W.-H. Sun, U. Thiele, S. Tokarz, Z. I. Tsvetanov, D. A. Turnshek, S. Veilleux, R. M. Wagner, S. J. Wagner, I. Wanders, T. Wang, W. F. Welsh, R. J. Weymann, R. J. White, B. J. Wilkes, B. J. Wills, C. Winge, H. Wu, Z. L. Zou, Steps toward determination of the size and structure of the broad-line region in active galatic nuclei. 8: An intensive HST, IUE, and ground-based study of NGC 5548. *Astrophys. J.* **97** (suppl.), 285 (1995). doi:10.1086/192144
8. A. Pancoast *et al*., arXiv:1311.6475 (2013).
9. G. Risaliti, M. Elvis, F. Nicastro, Ubiquitous variability of x-ray–absorbing column densities in Seyfert 2 galaxies. *Astrophys. J.* **571**, 234–246 (2002). doi:10.1086/324146
10. G. Lamer, P. Uttley, I. M. McHardy, An absorption event in the X-ray light curve of NGC 3227. *Mon. Not. R. Acad. Sci.* **342**, L41–L45 (2003). doi:10.1046/j.1365-8711.2003.06759.x
11. D. M. Crenshaw, S. B. Kraemer, Mass outflow from the nucleus of the Seyfert 1 galaxy NGC 4151. *Astrophys. J.* **659**, 250–256 (2007). doi:10.1086/511970
12. T. J. Turner, J. N. Reeves, S. B. Kraemer, L. Miller, Tracing a disk wind in NGC 3516. *Astron. Astrophys.* **483**, 161–169 (2008). doi:10.1051/0004-6361:20078808
13. S. Bianchi, E. Piconcelli, M. Chiaberge, E. J. Bailón, G. Matt, F. Fiore, How complex is the obscuration in active galactic nuclei? New clues from the *Suzaku* monitoring of the x-ray absorbers in NGC 7582. *Astrophys. J.* **695**, 781–787 (2009). doi:10.1088/0004-637X/695/1/781
14. G. Risaliti, G. Miniutti, M. Elvis, G. Fabbiano, M. Salvati, A. Baldi, V. Braito, S. Bianchi, G. Matt, J. Reeves, R. Soria, A. Zezas, Variable partial covering and a relativistic iron line in NGC 1365. *Astrophys. J.* **696**, 160–171 (2009). doi:10.1088/0004-637X/696/1/160
15. A. L. Longinotti, Y. Krongold, G. A. Kriss, J. Ely, L. Gallo, D. Grupe, S. Komossa, S. Mathur, A. Pradhan, The rise of an ionized wind in the narrow-line Seyfert 1 galaxy Mrk 335 observed by *XMM-Newton* and *HST*. *Astrophys. J.* **766**, 104 (2013). doi:10.1088/0004-637X/766/2/104
16. G. Miniutti, M. Sanfrutos, T. Beuchert, B. Agis-Gonzalez, A. L. Longinotti, E. Piconcelli, Y. Krongold, M. Guainazzi, S. Bianchi, G. Matt, E. Jimenez-Bailon, The properties of the clumpy torus and BLR in the polar-scattered Seyfert 1 galaxy ESO 323-G77 through X-ray absorption variability. *Mon. Not. R. Acad. Sci.* **437**, 1776–1790 (2014). doi:10.1093/mnras/stt2005
17. A. G. Markowitz, M. Krumpe, R. Nikutta, First X-ray-based statistical tests for clumpy-torus models: Eclipse events from 230 years of monitoring of Seyfert AGN. *Mon. Not. R. Acad. Sci.* **439**, 1403–1458 (2014). doi:10.1093/mnras/stt2492
18. D. Proga, T. R. Kallman, Dynamics of line-driven disk winds in active galactic nuclei. II. Effects of disk radiation. *Astrophys. J.* **616**, 688–695 (2004). doi:10.1086/425117
19. S. Gallagher, W. N. Brandt, G. Chartas, R. Priddey, G. P. Garmire, R. M. Sambruna, An exploratory *Chandra* survey of a well-defined sample of 35 large bright quasar survey broad absorption line quasars. *Astrophys. J.* **644**, 709–724 (2006). doi:10.1086/503762
20. D. M. Crenshaw, S. B. Kraemer, H. R. Schmitt, J. S. Kaastra, N. Arav, J. R. Gabel, K. T. Korista, Mass outflow in the Seyfert 1 galaxy NGC 5548. *Astrophys. J.* **698**, 281–292 (2009). doi:10.1088/0004-637X/698/1/281
21. L. Strüder, U. Briel, K. Dennerl, R. Hartmann, E. Kendziorra, N. Meidinger, E. Pfeffermann, C. Reppin, B. Aschenbach, W. Bornemann, H. Bräuninger, W. Burkert, M. Elender, M. Freyberg, F. Haberl, G. Hartner, F. Heuschmann, H. Hippmann, E. Kastelic, S. Kemmer, G. Kettenring, W. Kink, N. Krause, S. Müller, A. Oppitz, W. Pietsch, M. Popp, P. Predehl, A. Read, K. H. Stephan, D. Stötter, J. Trümper, P. Holl, J. Kemmer, H. Soltau, R. Stötter, U. Weber, U. Weichert, C. von Zanthier, D. Carathanassis, G. Lutz, R. H. Richter, P. Solc, H. Böttcher, M. Kuster, R. Staubert, A. Abbey, A. Holland, M. Turner, M. Balasini, G. F. Bignami, N. La Palombara, G. Villa, W. Buttler, F. Gianini, R. Lainé, D. Lumb, P. Dhez, The European Photon Imaging Camera on XMM-Newton: The pn-CCD camera. *Astron. Astrophys.* **365**, L18–L26 (2001). doi:10.1051/0004-6361:20000066
22. M. J. L. Turner, A. Abbey, M. Arnaud, M. Balasini, M. Barbera, E. Belsole, P. J. Bennie, J. P. Bernard, G. F. Bignami, M. Boer, U. Briel, I. Butler, C. Cara, C. Chabaud, R. Cole, A. Collura, M. Conte, A. Cros, M. Denby, P. Dhez, G. Di Coco, J. Dowson, P. Ferrando, S. Ghizzardi, F. Gianotti, C. V. Goodall, L. Gretton, R. G. Griffiths, O. Hainaut, J. F. Hochedez, A. D. Holland, E. Jourdain, E. Kendziorra, A. Lagostina, R. Laine, N. La Palombara, M. Lortholary, D. Lumb, P. Marty, S. Molendi, C. Pigot, E. Poindron, K. A. Pounds, J. N. Reeves, C. Reppin, R. Rothenflug, P. Salvetat, J. L. Sauvageot, D. Schmitt, S. Sembay, A. D. T. Short, J. Spragg, J. Stephen, L. Strüder, A. Tiengo, M. Trifoglio, J. Trümper, S. Vercellone, L. Vigroux, G. Villa, M. J. Ward, S. Whitehead, E. Zonca, The European Photon Imaging Camera on XMM-Newton: The MOS cameras. *Astron. Astrophys.* **365**, L27–L35 (2001). doi:10.1051/0004-6361:20000087
23. J. W. den Herder, A. C. Brinkman, S. M. Kahn, G. Branduardi-Raymont, K. Thomsen, H. Aarts, M. Audard, J. V. Bixler, A. J. den Boggende, J. Cottam, T. Decker, L. Dubbeldam, C. Erd, H. Goulooze, M. Güdel, P. Guttridge, C. J. Hailey, K. Al Janabi, J. S. Kaastra, P. A. J. de Korte, B. J. van Leeuwen, C. Mauche, A. J. McCalden, R. Mewe, A. Naber, F. B. Paerels, J. R. Peterson, A. P. Rasmussen, K. Rees, I. Sakelliou, M. Sako, J. Spodek, M. Stern, T. Tamura, J. Tandy, C. P. de Vries, S. Welch, A. Zehnder, The Reflection Grating Spectrometer on board XMM-Newton. *Astron. Astrophys.* **365**, L7–L17 (2001). doi:10.1051/0004-6361:20000058
24. J. S. Kaastra, C. P. de Vries, K. C. Steenbrugge, R. G. Detmers, J. Ebrero, E. Behar, S. Bianchi, E. Costantini, G. A. Kriss, M. Mehdipour, S. Paltani, P.-O.

Petrucci, C. Pinto, G. Ponti, Multiwavelength campaign on Mrk 509. *Astron. Astrophys.* **534**, A37 (2011). doi:10.1051/0004-6361/201116870
25. K. O. Mason, A. Breeveld, R. Much, M. Carter, F. A. Cordova, M. S. Cropper, J. Fordham, H. Huckle, C. Ho, H. Kawakami, J. Kennea, T. Kennedy, J. Mittaz, D. Pandel, W. C. Priedhorsky, T. Sasseen, R. Shirey, P. Smith, J.-M. Vreux, The XMM-Newton optical/UV monitor telescope. *Astron. Astrophys.* **365**, L36–L44 (2001). doi:10.1051/0004-6361:20000044
26. N. Gehrels, G. Chincarini, P. Giommi, K. O. Mason, J. A. Nousek, A. A. Wells, N. E. White, S. D. Barthelmy, D. N. Burrows, L. R. Cominsky, K. C. Hurley, F. E. Marshall, P. Meszaros, P. W. A. Roming, L. Angelini, L. M. Barbier, T. Belloni, S. Campana, P. A. Caraveo, M. M. Chester, O. Citterio, T. L. Cline, M. S. Cropper, J. R. Cummings, A. J. Dean, E. D. Feigelson, E. E. Fenimore, D. A. Frail, A. S. Fruchter, G. P. Garmire, K. Gendreau, G. Ghisellini, J. Greiner, J. E. Hill, S. D. Hunsberger, H. A. Krimm, S. R. Kulkarni, P. Kumar, F. Lebrun, N. M. Lloyd-Ronning, C. B. Markwardt, B. J. Mattson, R. F. Mushotzky, J. P. Norris, J. Osborne, B. Paczynski, D. M. Palmer, H.-S. Park, A. M. Parsons, J. Paul, M. J. Rees, C. S. Reynolds, J. E. Rhoads, T. P. Sasseen, B. E. Schaefer, A. T. Short, A. P. Smale, I. A. Smith, L. Stella, G. Tagliaferri, T. Takahashi, M. Tashiro, L. K. Townsley, J. Tueller, M. J. L. Turner, M. Vietri, W. Voges, M. J. Ward, R. Willingale, F. M. Zerbi, W. W. Zhang, The *Swift* Gamma-Ray Burst Mission. *Astrophys. J.* **611**, 1005–1020 (2004). doi:10.1086/422091
27. D. N. Burrows, J. E. Hill, J. A. Nousek, J. A. Kennea, A. Wells, J. P. Osborne, A. F. Abbey, A. Beardmore, K. Mukerjee, A. D. T. Short, G. Chincarini, S. Campana, O. Citterio, A. Moretti, C. Pagani, G. Tagliaferri, P. Giommi, M. Capalbi, F. Tamburelli, L. Angelini, G. Cusumano, H. W. Bräuninger, W. Burkert, G. D. Hartner, The Swift X-Ray Telescope. *Space Sci. Rev.* **120**, 165–195 (2005). doi:10.1007/s11214-005-5097-2
28. P. W. A. Roming, T. E. Kennedy, K. O. Mason, J. A. Nousek, L. Ahr, R. E. Bingham, P. S. Broos, M. J. Carter, B. K. Hancock, H. E. Huckle, S. D. Hunsberger, H. Kawakami, R. Killough, T. S. Koch, M. K. Mclelland, K. Smith, P. J. Smith, J. C. Soto, P. T. Boyd, A. A. Breeveld, S. T. Holland, M. Ivanushkina, M. S. Pryzby, M. D. Still, J. Stock, The Swift Ultra-Violet/Optical Telescope. *Space Sci. Rev.* **120**, 95–142 (2005). doi:10.1007/s11214-005-5095-4
29. F. A. Harrison, W. W. Craig, F. E. Christensen, C. J. Hailey, W. W. Zhang, S. E. Boggs, D. Stern, W. R. Cook, K. Forster, P. Giommi, B. W. Grefenstette, Y. Kim, T. Kitaguchi, J. E. Koglin, K. K. Madsen, P. H. Mao, H. Miyasaka, K. Mori, M. Perri, M. J. Pivovaroff, S. Puccetti, V. R. Rana, N. J. Westergaard, J. Willis, A. Zoglauer, H. An, M. Bachetti, N. M. Barrière, E. C. Bellm, V. Bhalerao, N. F. Brejnholt, F. Fuerst, C. C. Liebe, C. B. Markwardt, M. Nynka, J. K. Vogel, D. J. Walton, D. R. Wik, D. M. Alexander, L. R. Cominsky, A. E. Hornschemeier, A. Hornstrup, V. M. Kaspi, G. M. Madejski, G. Matt, S. Molendi, D. M. Smith, J. A. Tomsick, M. Ajello, D. R. Ballantyne, M. Baloković, D. Barret, F. E. Bauer, R. D. Blandford, W. N. Brandt, L. W. Brenneman, J. Chiang, D. Chakrabarty, J. Chenevez, A. Comastri, F. Dufour, M. Elvis, A. C. Fabian, D. Farrah, C. L. Fryer, E. V. Gotthelf, J. E. Grindlay, D. J. Helfand, R. Krivonos, D. L. Meier, J. M. Miller, L. Natalucci, P. Ogle, E. O. Ofek, A. Ptak, S. P. Reynolds, J. R. Rigby, G. Tagliaferri, S. E. Thorsett, E. Treister, C. M. Urry, The *Nuclear Spectroscopic Telescope Array* (*NuSTAR*) high-energy x-ray mission. *Astrophys. J.* **770**, 103 (2013). doi:10.1088/0004-637X/770/2/103
30. C. Winkler *et al.*, T. J.-L. Courvoisier, G. Di Cocco, N. Gehrels, A. Giménez, S. Grebenev, W. Hermsen, J. M. Mas-Hesse, F. Lebrun, N. Lund, G. G. C. Palumbo, J. Paul, J.-P. Roques, H. Schnopper, V. Schönfelder, R. Sunyaev, B. Teegarden, P. Ubertini, G. Vedrenne, A. J. Dean, The INTEGRAL mission. *Astron. Astrophys.* **411**, L1–L6 (2003). doi:10.1051/0004-6361:20031288
31. J. C. Green, C. S. Froning, S. Osterman, D. Ebbets, S. H. Heap, C. Leitherer, J. L. Linsky, B. D. Savage, K. Sembach, J. Michael Shull, O. H. W. Siegmund, T. P. Snow, J. Spencer, S. Alan Stern, J. Stocke, B. Welsh, S. Béland, E. B. Burgh, C. Danforth, K. France, B. Keeney, J. McPhate, S. V. Penton, J. Andrews, K. Brownsberger, J. Morse, E. Wilkinson, The Cosmic Origins Spectrograph. *Astrophys. J.* **744**, 60 (2012). doi:10.1088/0004-637X/744/1/60
32. B. J. Wills, H. Netzer, D. Wills, Broad emission features in QSOs and active galactic nuclei. II - New observations and theory of Fe II and H I emission. *Astrophys. J.* **288**, 94–116 (1985). doi:10.1086/162767
33. B. P. Wakker, F. J. Lockman, J. M. Brown, Measuring turbulence in the interstellar medium by comparing *N* (H I; Lyα) and *N* (H I; 21 cm). *Astrophys. J.* **728**, 159 (2011). doi:10.1088/0004-637X/728/2/159
34. TGCat data archive, http://tgcat.mit.edu.
35. J. S. Kaastra, R. Mewe, H. Nieuwenhuijzen, in *11th Colloquium on UV and X-ray Spectroscopy of Astrophysical and Laboratory Plasmas*, K. Yamashita, T. Watanabe, Ed. (Univ. Acad. Press, Tokyo, 1996), pp. 411-414.
36. SPEX website www.sron.nl/spex.
37. K. Lodders, H. Palme, *Meteorit. Planet. Sci.* **44** (suppl.), abstract no. 5154 (2009).
38. G. J. Ferland *et al.*, *Rev. Mex. Astron. Astrof.* **49**, 1–27 (2013).

Acknowledgments: The data used in this research are stored in the public archives of the international space observatories involved: XMM-Newton, HST, Swift, NuSTAR, INTEGRAL and Chandra. We acknowledge support by ISSI in Bern; the Netherlands Organization for Scientific Research; NASA HST program 13184 from STScI, which is operated by AURA, Inc., under NASA contract NAS5-26555; the UK STFC; the French CNES, CNRS/PICS and CNRS/PNHE; VRIDT (Chile); Israel's MoST, ISF (1163/10), and I-CORE program (1937/12); the Swiss SNSF; the Italian ASI grant INAF I/037/12/0-011/13 and INAF/PICS; US NSF grant AST-1008882; EU Marie Curie contract FP-PEOPLE-2012-IEF-331095. We thank Silvana Paniagua for helping with Fig. 4.

Supplementary Materials
www.sciencemag.org/cgi/content/full/science.1253787/DC1
Materials and Methods
Figs. S1 to S4
Tables S1 to S3
References (*21–38*)
Movie S1

24 March 2014; accepted 09 June 2014
Published online 19 June 2014
10.1126/science.1253787

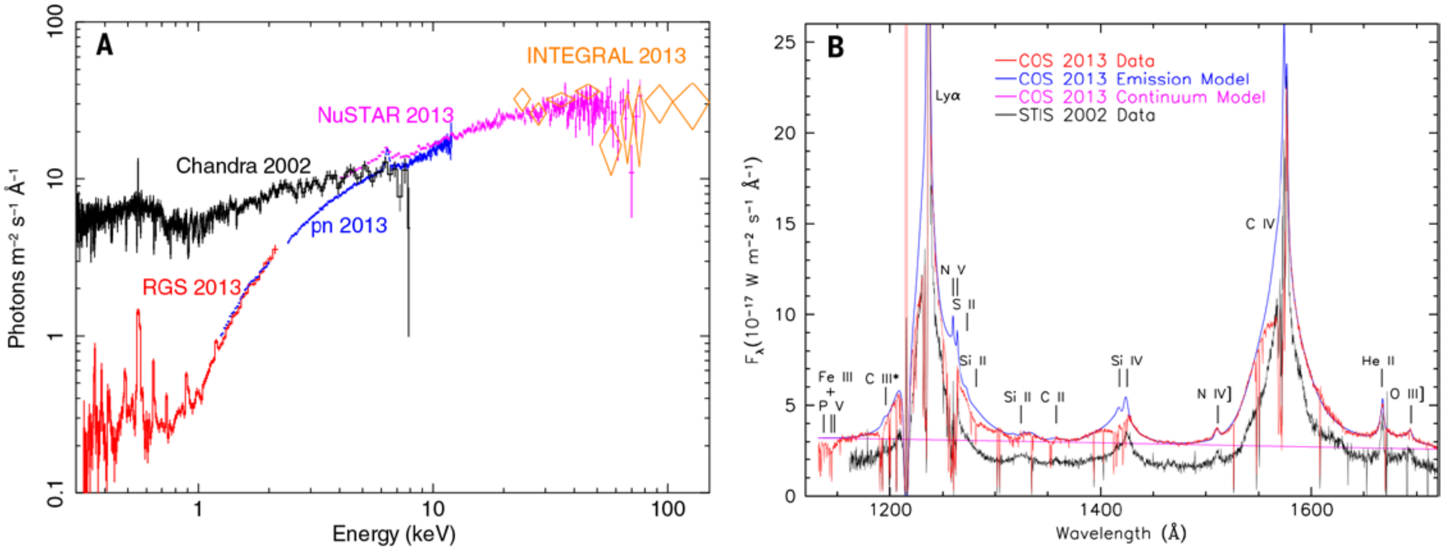

Fig. 1. X-ray and UV spectra of NGC 5548. All data have been rebinned for clarity. Error bars are ±1 SD. (**A**) The heavily obscured X-ray spectrum during summer 2013. The unobscured Chandra Low Energy Transmission Grating Spectrometer (LETGS) spectrum taken in 2002 is shown for comparison. The 2013 spectrum is obtained from 12 XMM-Newton observations (EPIC-pn detector (pn) and Reflection Grating Spectrometers (RGS)), two NuSTAR and four INTEGRAL observations; these latter two datasets were taken when the hard X-ray flux was 10% higher than the average >10 keV flux of the XMM-Newton data. (**B**) Averaged 2013 Cosmic Origins Spectrograph (COS) spectrum compared to 2002 Space Telescope Imaging Spectrograph (STIS) spectrum, showing the broad UV absorption lines in 2013.

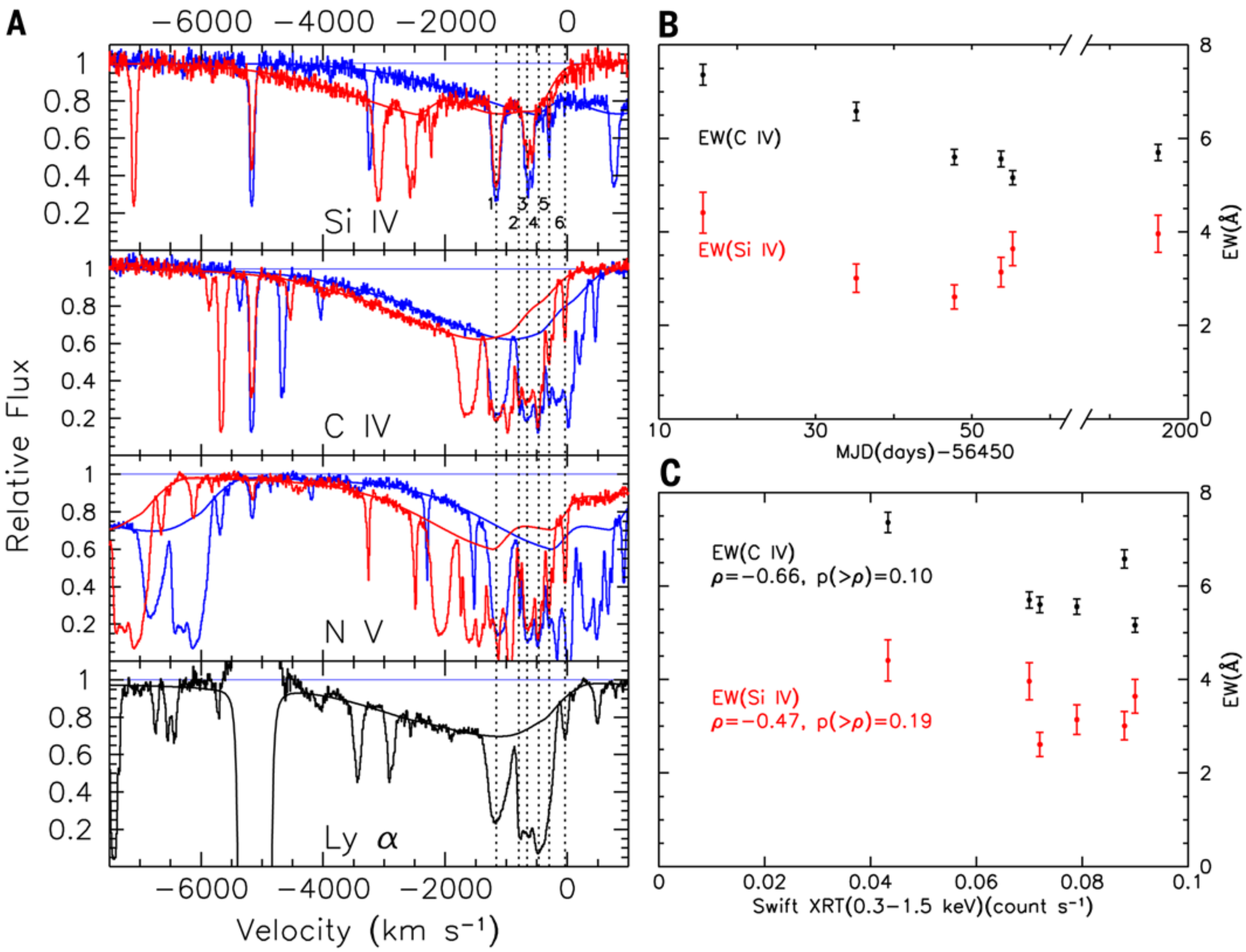

Fig. 2. UV absorption lines in the COS spectrum of NGC 5548. (**A**) The combined normalized spectra from summer 2013 have been binned for clarity. For the Si IV, C IV, and N V doublets, the red and blue profiles are registered relative to the respective red and blue wavelengths of the doublets. The smooth solid lines are fits to the broad absorption line profile with 1:1 ratio for the doublets. The dotted vertical lines show the locations of the narrow velocity components defined in (*20*), with an additional component 6 near 0 velocity. (**B**) Time variability of the equivalent width (EW) of the C IV and Si IV broad absorption troughs (including the 2014 measurement). Error bars are ±1 SD. (**C**) Equivalent widths of the C IV and Si IV broad absorption troughs, showing an anti-correlation with the Swift soft X-ray flux (0.3−1.5 keV). Error bars are ±1 SD.

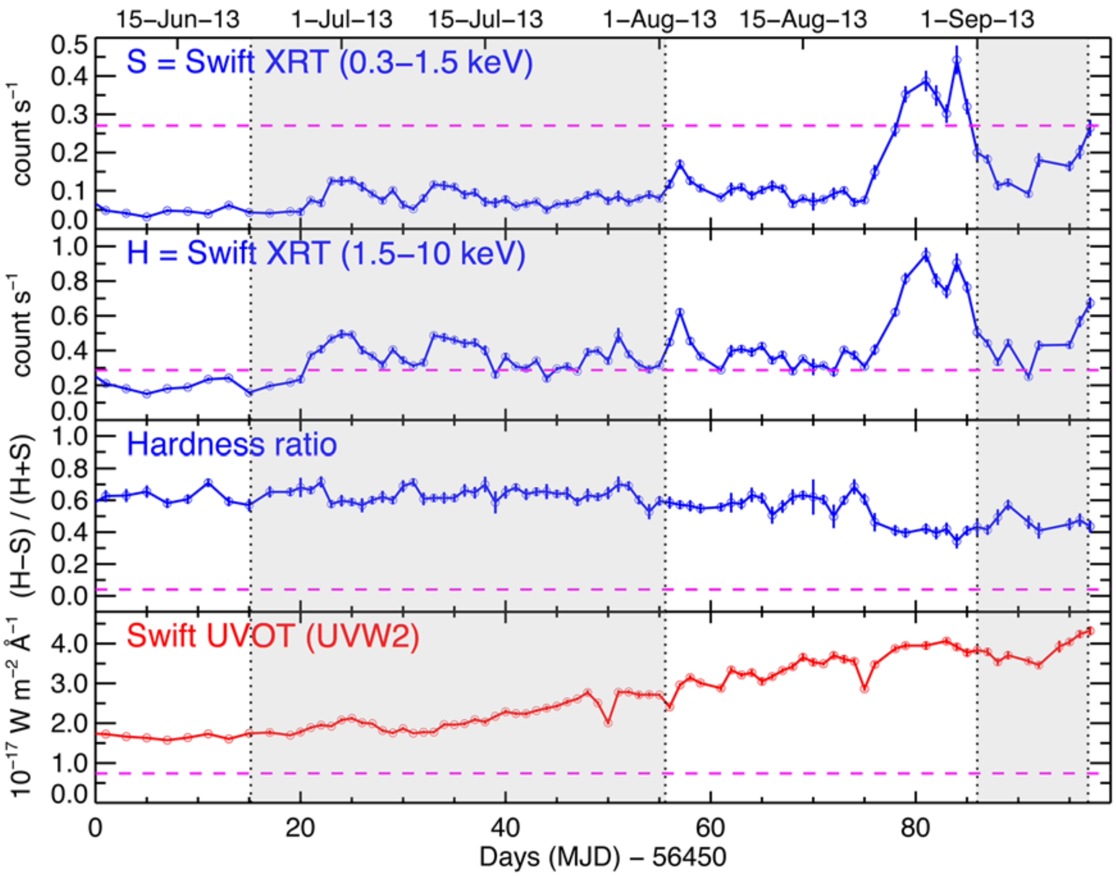

Fig. 3. X-ray and UV light curves of NGC 5548 obtained with Swift. Horizontal dashed lines show the average flux or hardness measured with Swift during 2005 and 2007 in an unobscured state. The first and second shaded areas indicate the epochs of the first 12 XMM-Newton and the three Chandra observations, respectively. The outburst around day 80 was also obscured, as evidenced by the hardness ratio. Note the apparent anti-correlation between hardness and UV flux. Error bars are ±1 SD. The full light curve is shown in Fig. S4.

Fig. 4. Cartoon of the central region of NGC 5548 (not to scale). The disk around the black hole (BH) emits X-ray, UV, optical and IR continuum and is surrounded by a dusty torus. The curved lines indicate the outflow of gas along the magnetic field lines of an accretion disk wind. The obscurer consists of a mixture of ionized gas with embedded colder, denser parts and is close to the inner UV broad emission line region (BLR). The narrow line region (NLR) and the persistent warm absorber (WA) are farther out.